Fermi National Accelerator Laboratory

FERMILAB-Conf-95/041

Charm Photoproduction Dynamics

Peter H. Garbincius

Fermi National Accelerator Laboratory
P.O. Box 500, Batavia, Illinois 60510

March 1995

Presented at the *LAFEX International School in High Energy Physics, Centro Brasiliero de Pesquisas Fisicas (CBPF),* Rio de Janeiro, Brazil, February 20, 1995

Disclaimer

Charm Photoproduction Dynamics

Peter H. Garbincius

Fermi National Accelerator Laboratory

Batavia, IL 60510 U.S.A.

Summary. - Photoproduction of open charm is reviewed, both as a tool for studying the properties of charm particles such as spectroscopy, decays, and lifetimes, and as a testing ground for theoretical calculations of production dynamics. Many characteristics of charm photoproduction are described in terms of the leading order (LO) $\alpha_{EM}\alpha_S$ Photon-Gluon Fusion (PGF) model. The next-to-leading order (NLO) corrections of strength $\alpha_{EM}\alpha_S^2$ due to radiation of additional gluons are then added. The sensitivities of the NLO calculations on the mass of the charm quark, m_c, and on the choice of the gluon structure function of the nucleon are illustrated for the energy dependence of the cross section for charm photoproduction. These are compared with fixed target data and new HERA data. The single charm particle inclusive distributions in x_f and $p_\perp^2$, along with $\sigma(\gamma N \to c\bar{c}X)$ give good estimates of m_c and n_g, the shape parameter for the gluon distribution within the nucleon. As in hadroproduction, some disagreements between prediction and observation begin to appear in trying to simultaneously match the distributions in both $p_\perp^2$ for single charm particles and in the $\Delta\Phi$ acoplanarity angle between pairs of charm particles. These can be partially remedied by modifying the fragmentation function for c-quarks into charm particles, and by including extra $k_\perp^2$ transverse smearing of the gluon distributions within the target nucleon. Initial studies of the relative production between charm particles and anti-particles indicate disagreement with the predictions of the independent string fragmentation model.

1 Why study photoproduction?

In studying uncommon phenomena, such as charm quark physics, there is always a conflict as to the best way to optimize the output of a given experiment. The choice of photoproduction of charm, rather than production by either proton or pion beams has the following advantages. First, at typical fixed target energies, the relative rate of interactions producing charm particles to the total rate of producing multi-particle hadronic final states is about 0.6 % in photoproduction, while it is only about 0.08 % with hadron beams. Second, the photon predominantly acts as a $x = 1$ parton or constituent and produces relatively higher momentum charm particles which is more closely matched to acceptances of spectrometers and giving larger Lorentz boosts to allow observation of charm particle lifetimes and discrimination of charm signals from backgrounds by cutting on the significance of separation of secondary charm decay vertices. Photoproduction has relative disadvantages also. The photoproduced events are cleaner, often too clean to find the primary interaction vertex! Photoproduction events are always luminosity limited, requiring the use of thicker, non-point targets, leading to increased multiple scattering and secondary interactions and compromised acceptances of the vertex detectors. Thick radiators are often used,

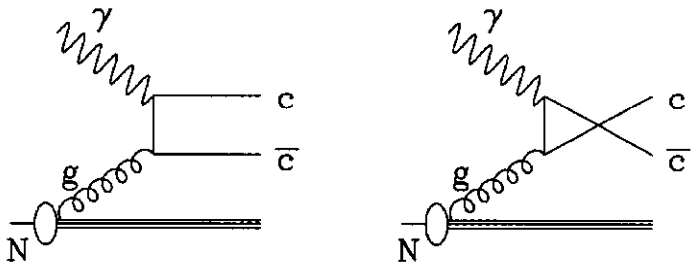

Figure 1: Leading Order $\alpha_{EM}\alpha_S$ Photon Gluon Fusion Graphs.

leading to multiple bremsstrahlung and backgrounds from $\gamma \rightarrow e^+e^-$ conversions. Finally, the neutral γ beam leaves no incident beam track to guide the reconstruction programs by seeding the primary vertex.

The underlying dynamics of charm photoproduction are quite interesting theoretically in their own right and can be used to study the mass of the charm quark, gluon structure of the nucleon, and QCD systematics.

2 Theoretical introduction

Photoproduction dynamics are much simpler than for hadroproduction of charm. The primary graph is the Photon Gluon Fusion (PGF) model where the photon behaves like an $x = 1$ parton contributing its full energy to the interaction. Theoretical calculations are available for leading order (LO) and next-leading-order (NLO) processes, along with contributions where the photon dissociates into hadronic components before interacting. This resolved photon process, which more closely resembles hadroproduction, is anticipated to be a non-negligible contribution only at HERA energies.

The leading order PGF process is described in Reference [1] and illustrated in Figure 1. The incident photon simply inteacts with a gluon from the target nucleon producing a $c\bar{c}$ pair. The theoretical predictions of $\sigma(\gamma N \rightarrow c\bar{c}X)$ and the x_f distribution of the c and $\bar{c}$ quarks depends on the QCD couplings and evolution, both of which depend on the m_c, the mass of the charm quark, and the nucleon structure functions. The minimum momentum fraction x_g of a gluon within a nucleon to produce a $c\bar{c}$ pair is $x_g > M^2_{c\bar{c}}/2M_pk$, where k is the photon energy in the nucleon rest frame. Thus charm photoproduction samples the gluon distribution for $x_g > 0.04$ at typical fixed target energies and for $x_g > 0.00016$ at typical HERA energies. These graphs contribute to the order of $\alpha_s\alpha_{EM}$. To get from the $c\bar{c}$ distributions to those for observable charm particles, the fragmentation functions must be folded in. As we shall see, there will also be the continuing question of intrinsic transverse momentum of the gluon within the target nucleon. An example of a LO PGF event generator for simulating experiments and calculating acceptances and efficiencies is that of the Lund/PYTHIA monte carlo [2] which includes the hard

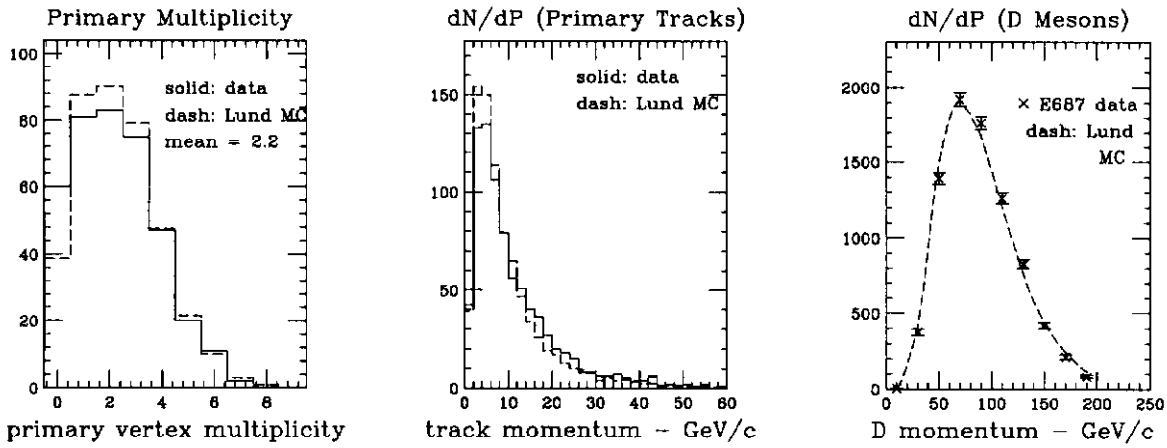

Figure 2: Observations of some distributions as observed in Fermilab E-687 compared to predictions of Lund model.

scattering LO PFG matrix element, a primordial gluon transverse momentum distribution with $< k_\perp >= 440$ MeV/c, ELQH nucleon structure function (other choices available), independent string fragmentation, and initial and final state showers (LLA). Some examples of experimental distributions from Fermilab E-687 and corresponding Lund simulations are illustrated in Figure 2.

The complication of additional radiated gluons, Figure 3, is treated to next leading order of $\alpha_{EM}\alpha_S^2$ by the authors of References [3, 4, 5, 6, 7]. The final state $Q\overline{Q}q$ and $Q\overline{Q}\overline{q}$ graphs involving virtual gluon exchange must be included to cancel divergences in the external gluon radiation graphs. At the energies of fixed target experiments, the NLO corrections are typically 20-30 % of the LO terms.

Finally, the photon itself may interact as a hadron, resolving itself into quark and gluon components before interacting with the gluon [8]. This process is related to vector dominance models of photoproduction, and to the photon structure functions as measured in $\gamma - \gamma$ interactions. The resolved photon component is calculated to be small at fixed target energies, but may contribute at the 30 - 50 % level at HERA energies, depending on the choice of $G_\gamma(x)$ structure function.

3 Charm photoproduction predictions and data

3.1 $c\bar{c}$ Cross Sections

Figure 4 displays the LO, NLO, and resolved photon contributions to $\sigma(\gamma N \rightarrow c\bar{c}X)$ for fixed target photoproduction energies, along with sensitivities to choice of m_c charm quark mass and structure function. The data and curves are from References [3, 4, 5, 6].

There are three high statistics experiments studying charm photoproduction dynamics. Fermilab E-691 [9, 10], CERN NA-14/2 [11], and Fermilab E-687 study systematics of single charm particle photoproduction, while NA-14/2 [12] and E-687 [13, 14] also study correlations between photoproduced pairs of charm particles. Typical data samples are 11,000 charm particles (E-691), 650 charm particles (NA-14/2), 22 $c\bar{c}$ pairs (NA-14/2), and 325 $c\bar{c}$ pairs (E-687). E-687

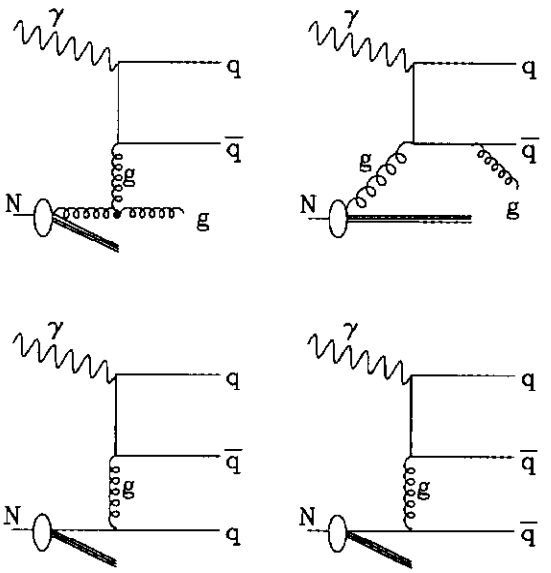

Figure 3: Next-to-Leading Order $\alpha_{EM}\alpha_S^2$ Photon Gluon Fusion Graphs.

has approximately 100,000 charm particles reconstructed with $< E_\gamma > \approx$ 200 GeV, with $\approx$ 60% good energy tags, but has not yet completed the $\sigma(\gamma N \rightarrow c\bar{c}X)$ or single charm particle analyses.

Recently, charm photoproduction (low Q^2 electroproduction) results have become available from the two HERA experiments, ZEUS [15] and H1 [16]. ZEUS reconstructs the decay chain $D^{*+} \rightarrow \pi^+ D^0$ followed by $D^0 \rightarrow K^-\pi^+$. Due to the correlation between the single K^- and the two $\pi^+\pi^+$ charges, further particle identification is not required. ZEUS observes 48 $\pm$ 11 photoproduced $D^{*\pm}$ particles, Figure 5, and an additional $\approx$ 16 D^* electroproduced with $Q^2 >$ 4 GeV^2. Although H1 also has a comparable D^* sample, they quote their photoproduction cross section based on observation of single inclusive $\mu^\pm$ production. These HERA experiments only have acceptance over about 10 % of the kinematic range for charm particle production and rely on theoretical extrapolation, with concurrent systematic uncertainties, to quote total $c\bar{c}$ cross sections. The cross sections are plotted in Figure 6, along with NLO predictions for a range of parameters. Even with such small number of charm events, the HERA experiments provide a very long lever arm to help limit the range of suitable parameters.

4 m_c and n_g from x_f and $p_\perp^2$ distributions

Simultaneously fitting $\sigma_{c\bar{c}}(k)$, $d\sigma/dx_f$, and $d\sigma/dp_\perp^2$, both E-691 [10] and NA14/2 [11] evaluate the mass of the charm quark and ths shape of the gluon distribution within the nucleon. They find $m_c = 1.74^{+0.13}_{-0.18}$ GeV (E-691), and $m_c = 1.5^{+0.2}_{-0.1}$ GeV (NA-14/2). For the gluon distribution in the nucleon target, NA-14/2 uses $xG(x) = (1-x)^{n_g}$ and finds $n_g = 5.3^{+2.3}_{-1.0}$, while E-691 uses the slightly different form $G(x) = (1-x)^{n_g}$ and finds $n_g = 7.1 \pm 2.2$.

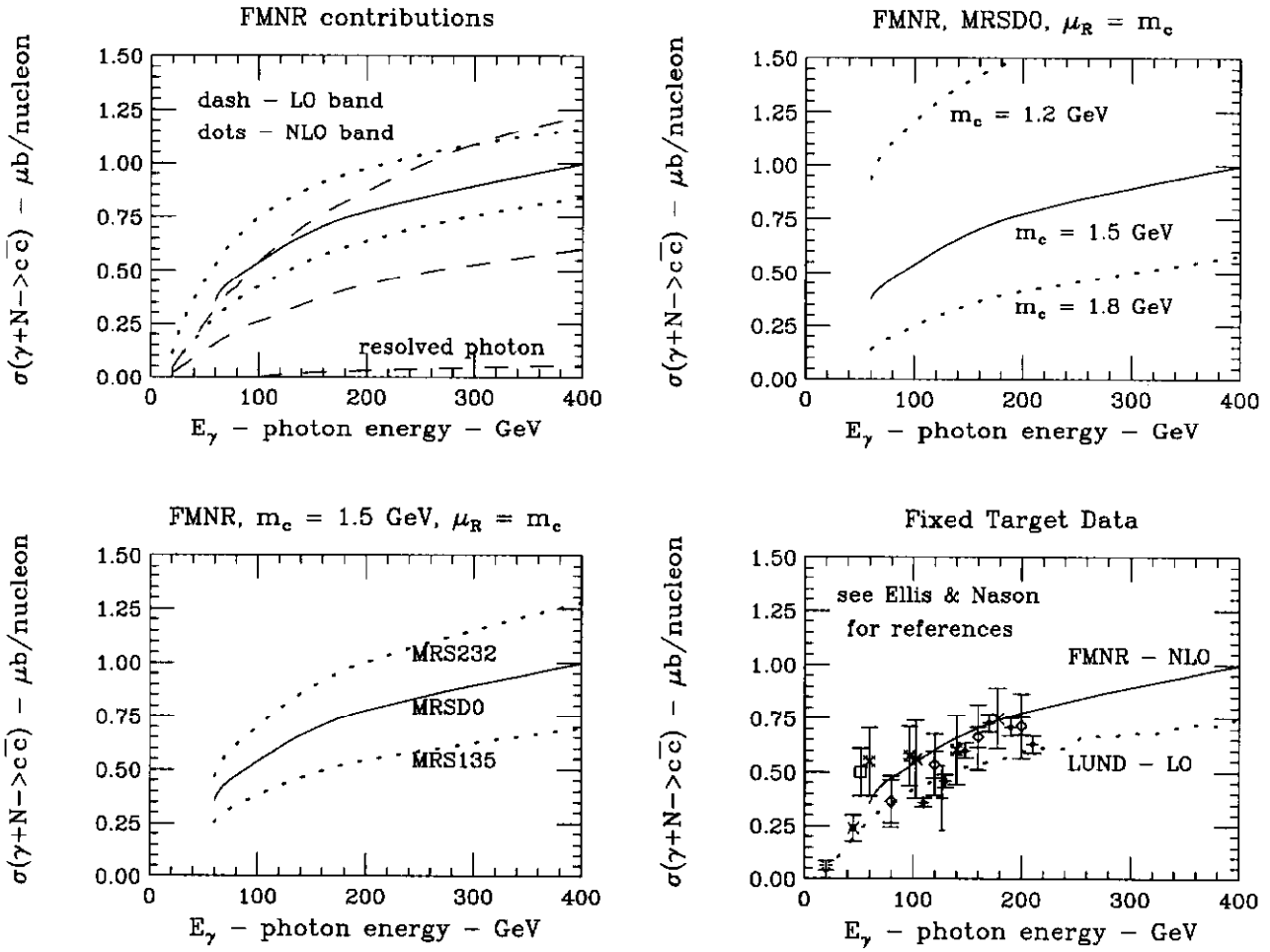

Figure 4: Calculated energy dependence of $\sigma(\gamma N \to c\bar{c}X)$ at fixed target energies for LO, NLO, and resolved photon components, variations with m_c, and variations with choice of structure function, for comparison with data.

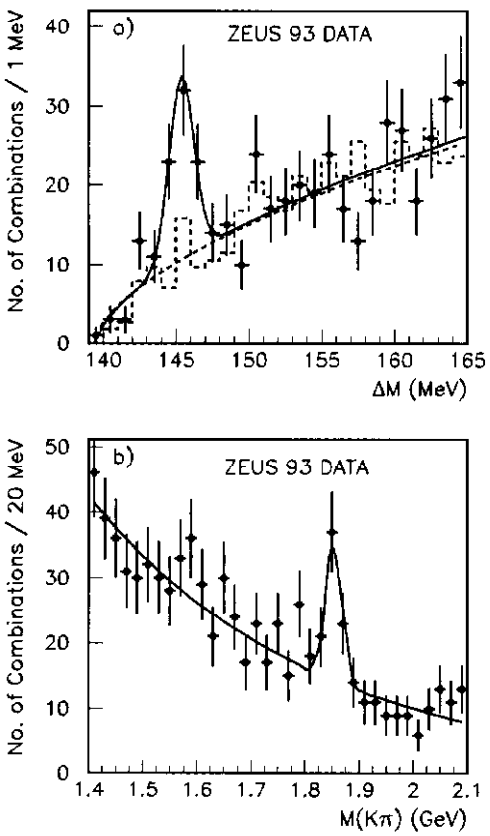

Figure 5: D* signals from ZEUS: $\Delta M = M(\pi^+K^-\pi^+) - M(K^-\pi^+)$ for events in D^0 peak along with wrong charge combination background, and $M(K^-\pi^+)$ for events in ΔM peak.

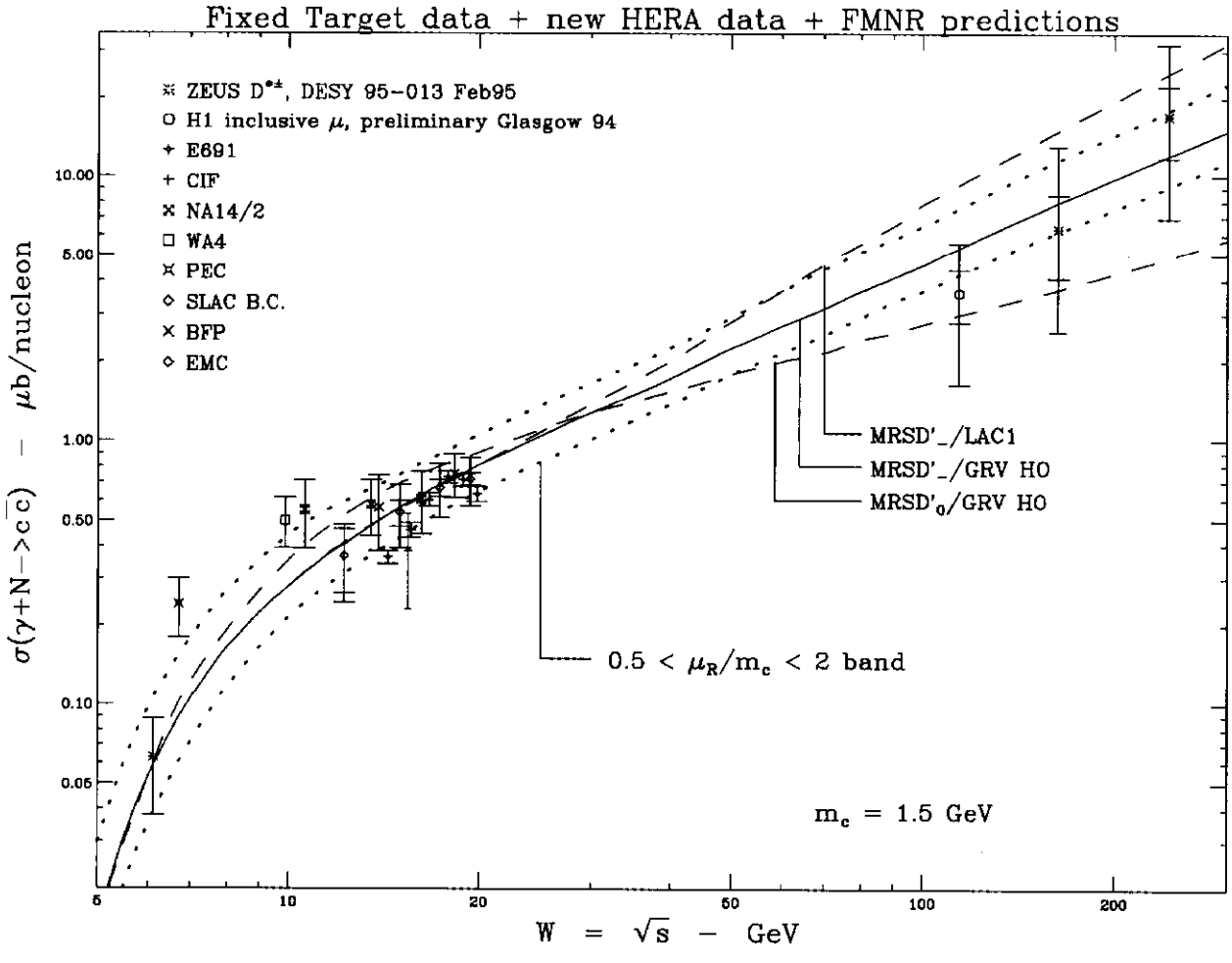

Figure 6: Recent HERA charm photoproduction cross sections from ZEUS and H1 compared to FMNR NLO predictions for a range of structure functions and renormalization masses.

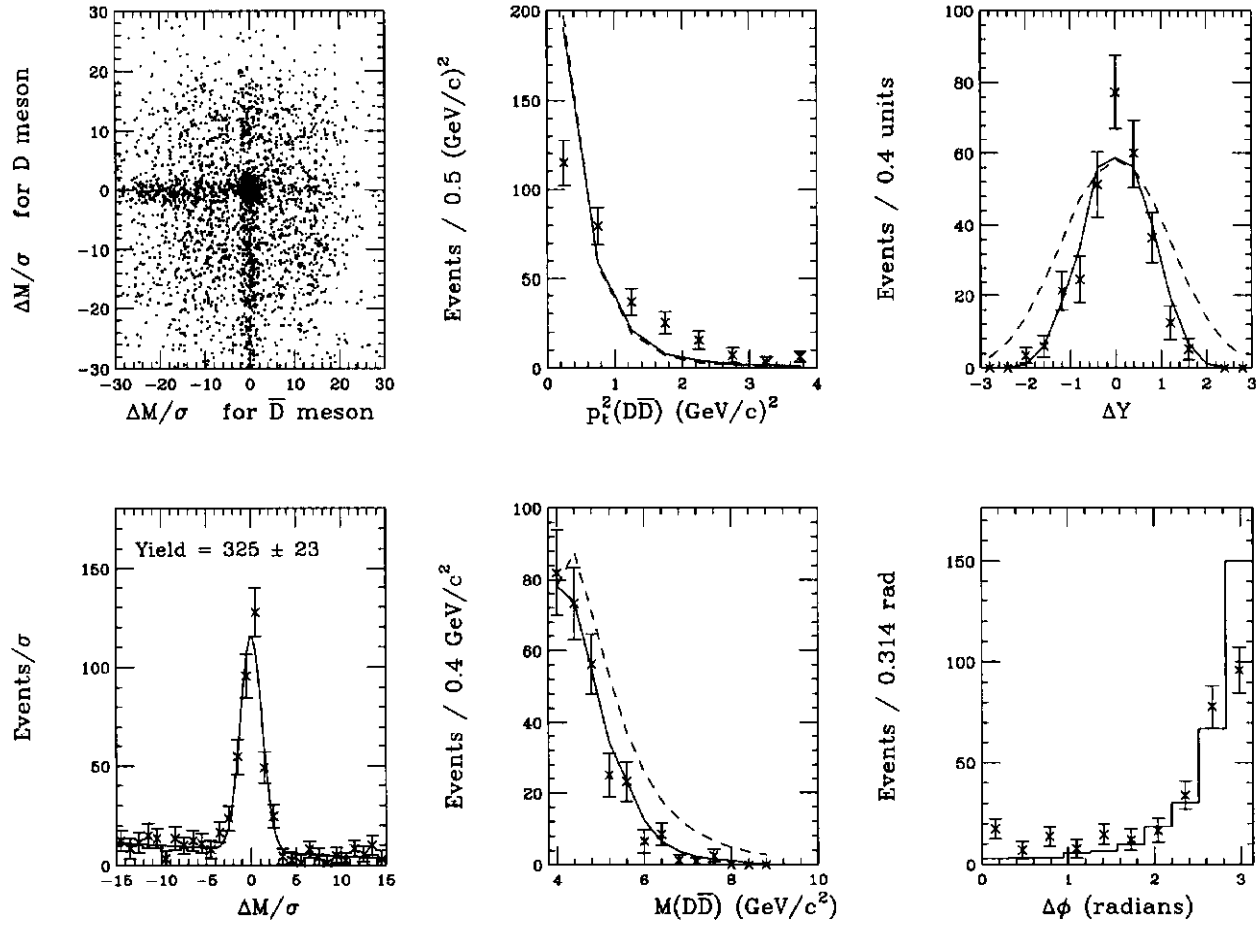

Figure 7: Correlations between $D\overline{D}$ pairs from E-687. The dashed curves are the generated predictions of the Lund monte carlo, before applying the experiment efficiencies and acceptances, while the solid curves are the Lund predictions including these efficiencies and acceptances and are thus directly comparable to the data points.

4.1 Correlations and intrinsic gluon $k_\perp^2$

E-687 [13, 14] and NA14/2 [12] have data sets where both the charm and anti-charm particles are reconstructed in the same event. These events use the majority decay channels $D^+ \rightarrow K^-\pi^+\pi^+, D^0 \rightarrow K^+\pi^-$, and $D^0 \rightarrow K^-\pi^+\pi^-\pi^+$ and the charge conjugate states. Typical correlated mass spectra and the distributions in the variables $M(D\overline{D})$, $p_\perp^2(D\overline{D})$, ΔY, and $\Delta\Phi$, where ΔY is the difference in the rapidities and $\Delta\Phi$ is the difference in azimuthal angle between the $D\overline{D}$ pair are shown in Figure 7.

Although the $M(D\overline{D})$ and ΔY data distributions agree well with the LO PGF Lund predictions, the $p_\perp^2(D\overline{D})$ and acoplanarity $\Delta\Phi$ distributions do not. This could be an indication of additional intrinsic $k_\perp^2$ momentum of the gluons within the target nucleus. In order to get agreement between the data and LO prediction, an additional amount of gluon transverse momentum corresponding to $< k_\perp^2 > \approx 0.5\ GeV^2$ is required for the $\Delta\Phi$ and $< k_\perp^2 > \approx 1\ GeV^2$. for the $p_\perp^2(D\overline{D})$ distributions [6]. These are surprisingly large relative to the nucleon rest mass.

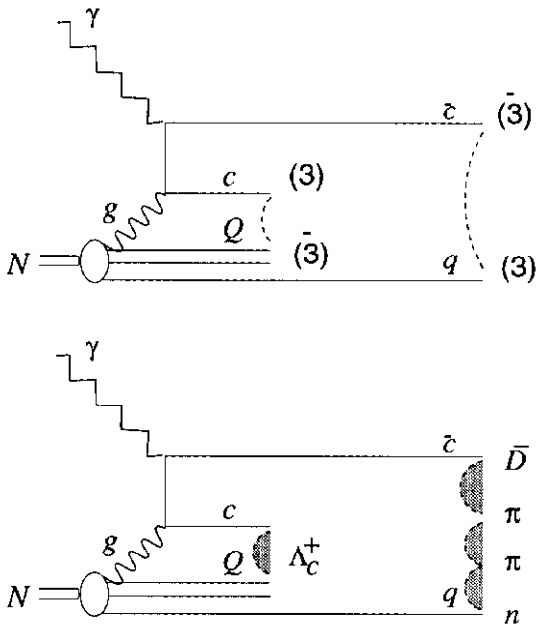

Figure 8: The independent string fragmentation model where the color of the photon-gluon system is compensated through string correlations with the remaining nucleon fragments.

4.2 Asymmetries and Fragmentation

The final photoproduction dynamics topic involves fragmentation. After the $c\bar{c}$ pair is produced, it must dress itself into the common charm hadrons we observe in experiments, as in Figure 8. The $c\bar{c}$ pair cannot simply form a fragmentation string in isolation as for the e^+e^- annihilation case. That would lead to a color non-singlet final state since the the $c\bar{c}$ system has the color of the exchanged gluon. There must be some color exchange with the remaining target remnants. The Lund string fragmentation model [2] has the c and the $\bar{c}$ quarks forming color singlet strings with the quark, anti-quarks, and di-quarks among the target nucleon remnants. This scheme solves a potential color match problem for the photon gluon fusion model and makes definite predictions for correlations and production ratios among the produced charm mesons, anti-charm mesons, and charm baryons. For example, the c quark could easily find a remnant di-quark leading to states with a charm baryon and a forward $\overline{D}$ meson. This could produce an observable asymmetry

$$\alpha = \frac{N(c) - N(\bar{c})}{N(c) + N(\bar{c})}$$

for D mesons. Such an asymmetry due to $\overline{D}\Lambda_c$ correlation is observed as anticipated at low energies, near $c\bar{c}$ photoproduction threshold.

Three experiments E-687 [14], E-691 [9], and NA14/2 [12] all have observed such asymmetries. However, it must be noted that these are measured as the integral over the physics quantaties modified by the individual experiment's acceptances, efficiencies, and kinematic ranges. Therefore, comparisons between experiments can only be indicative of a trend and such comparisons of raw distributions must be made with caution. E-687 has taken the Lund string fragmentation model monte carlo and run its predictions through the E-687 experiment simu-

lation in order to produce predicted asymmetries that can be directly compared to the E-687 observations. These asymmetries integrated over the experiment are listed in Table 1.

Table 1. Charm particle production asymmetries (in %) observed for the E-687 experimental conditions compared to Lund predictions for those same experimental conditions. The E-691 observations (different experimental conditions) are shown without comparison to predictions.

Decay mode	E-687	Lund	E-691
$D^+ \to K^-\pi^+\pi^+$	-3.8 ± 0.9 %	-12.7 ± 0.9 %	-2.0 ± 1.5 %
$D^{*+} \to \pi^+(D^0 \to K^-\pi^+)$	-6.4 ± 1.5 %	-10.8 ± 0.9 %	-7.0 ± 3.5 %
$D^{*+} \to \pi^+(D^0 \to K^-\pi^+\pi^-\pi^+)$	-4.0 ± 1.7 %	-11.5 ± 1.0 %	-10.3 ± 2.8 %
$D^0 \to K^-\pi^+$ $(no\ tag)$	-2.0 ± 1.5 %	-3.6 ± 0.6 %	-3.8 ± 1.5 %
$D^0 \to K^-\pi^+\pi^-\pi^+$ $(no\ tag)$	-1.9 ± 1.5 %	-6.9 ± 0.7 %	-
$D_s^+ \to K^-K^+\pi^+$	2.5 ± 5.2 %	4.8 ± 0.1 %	4.2 ± 6.8 %
$\Lambda_c^+ \to pK^-\pi^+$	3.5 ± 7.6 %	17.4 ± 1.6 %	11.7 ± 8.4 %

Averaging over D meson states, E-687 finds $\alpha = -3.7 \pm 0.6$ %. Similarly, NA14/2 finds $\alpha = -3 \pm 5$ % for D^+ and D^{*+}, and $\alpha = 24 \pm 17$ % for D_s^+. Since the kinematic ranges are different between all experiments, it is difficult to directly compare. In order to further compare the kinematical variations of Lund predictions and observed data, E-687 has plotted their asymmetry data as functions of the photon energy E_γ, $p_\perp^2$, and x_f in Figure 9. Although the data follow the general trends of the Lund independent string fragmentation model, the observed asymmetries are considerably smaller than those predicted, possibly indicating that other schemes may be also operative.

5 Conclusions

In this brief review of the phenomenology of charm photoproduction, we have seen that the LO and NLO calculations using the photon gluon fusion model seem to be reasonable for $\sigma(\gamma N \to c\bar{c}X)$ and in this context, the single charm particle inclusive distributions in x_f and $p_\perp^2$ can give the mass of the charm quark and the gluon distributions within the nucleon target. Fitting of the the $p_\perp^2$ and $\Delta\Phi$ distributions for $c\bar{c}$ pairs requires relatively large amounts of additional gluon $k_\perp^2$ smearing. There still reamins a large amount of predictive freedom due to the wide choices of the structure functions and QCD mass scales. The longer lever arm of the HERA data and higher precision results from E-687 will help pin down these choices and better test NLO QCD. Detailed comparisons of the predictions and observations for production asymmetries and correlations are just beginning.

6 Acknowledgements

I would like to thank all my colleagues and friends, some old, some new, who shared their data, insights, and understanding. These especially include: Keith Ellis, Daniel Treille, Patrick Roudeau, Milind Purohit, Joel Feltesse, Malcolm Derrick, Jit Ning Lim, Jesus Roldan, Zeyuan Wu, and Rob Gardner.

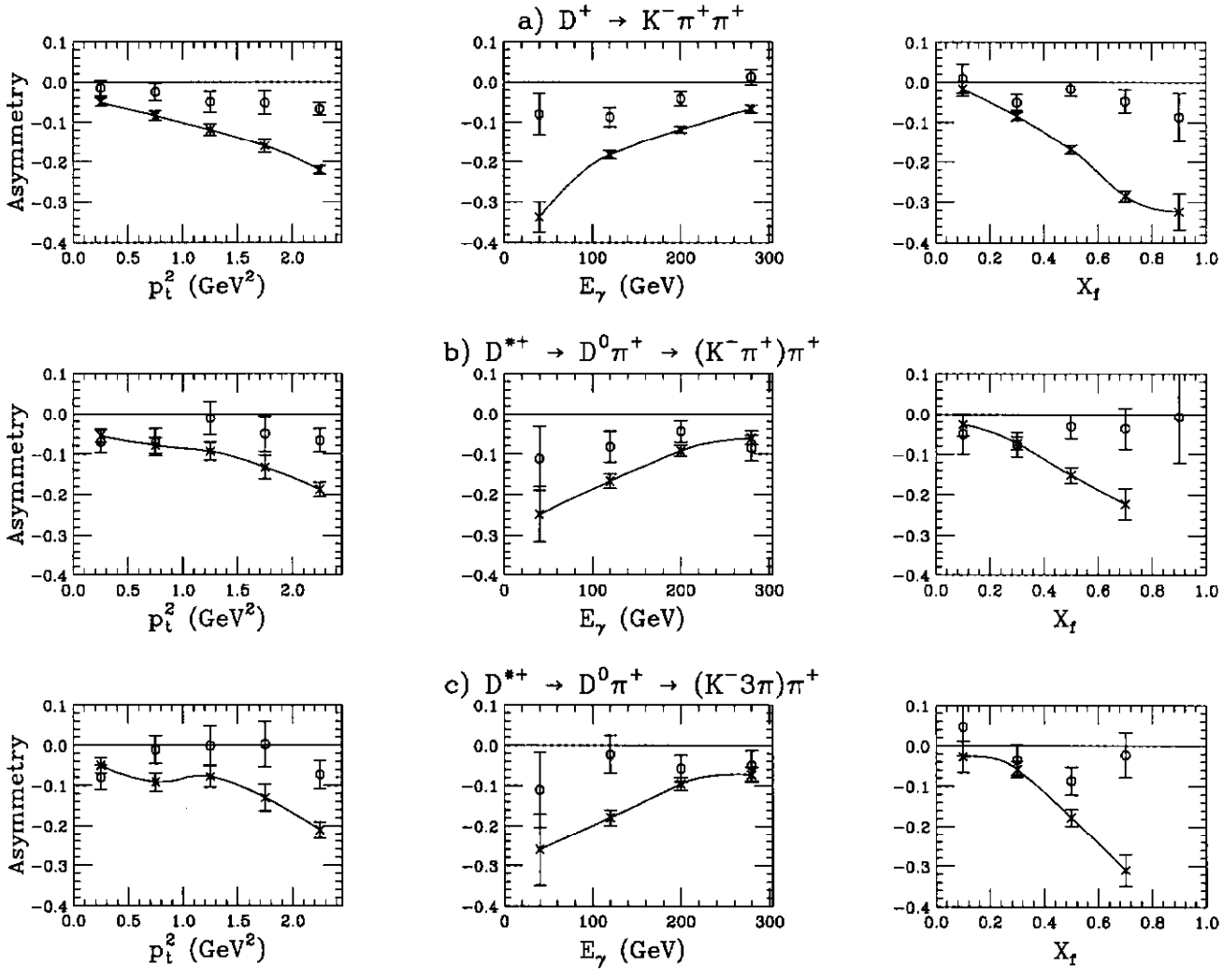

Figure 9: Variation of production asymmetries observed in E-687 and the corresponding Lund string fragmentation predictions for D^+ and two modes of D^{*+} as function of $p_\perp^2$, E_γ, and x_f.

References

[1] L.M. Jones and H.W. Wyld, Charmed-particle production by photon-gluon fusion, *Phys. Rev.* **D 17**, 759 (1978).

[2] T. Sjöstrand, The Lund Monte Carlo for Jet Fragmentation and e^+e^- Physics - JETSET Version 6.2, *Computer Phys. Commun.* **39** (1968) 347; T. Sjöstrand and M. Bengtsson, The Lund Monte Carlo for Jet Fragmentation and e^+e^- Physics - JETSET Version 6.3 - an Update, *Computer Phys. Commun.* **43** (1987) 367; and H.-U. Bengtsson and T. Sjöstrand, The Lund Monte Carlo for Hadronic Processes - PYTHIA Version 4.8, *Computer Phys. Commun.* **46** (1987) 43.

[3] R.K. Ellis and P. Nason, QCD Radiative Corrections to the Photoproduction of Heavy Quarks, *Nucl. Phys.* **B 312** (1989) 551.

[4] S. Frixione, M. Mangano, P. Nason, and G. Ridolfi, Heavy Quark Correlations in Photon-Hadron Collisions, *Nucl. Phys.* **B 412** (1994) 225.

[5] P. Nason, S. Frixione, M. Mangano, and G. Ridolfi, Heavy Flavor Production in Perturbative QCD, Advanced Study Conference on Heavy Flavours, Pavia, Italy, September, 1993, edited by G. Bellini, L. Brogiato, J. Butler, M. Giammarchi, and S. Ratti, Editions Frontieres, Gif-sur-Yvette Cedex - France, 1994, page 139.

[6] S. Frixione, M. Mangano, P. Nason, and G. Ridolfi, Charm and Bottom Production: Theoretical Results Versus Experimental Data, *Nucl. Phys.* **B431** (1994) 453.

[7] J. Smith and W.L. van Neerven, QCD corrections to heavy flavour photoproduction and electroproduction, *Nucl. Phys.* **B 374** (1992) 36.

[8] E. Witten, Anomolous cross sections for photon-photon scattering in gauge theories, *Nucl. Phys.* **B 120** (1977) 189; J.F. Owens, Photoproduction of large-transverse-momentum hadronic jets, *Phys. Rev.* **D 21**, 54 (1980); M. Drees and F. Halzen, Hadron Structure of High-Energy Photons, *Phys. Rev. Lett.* **61**, 275 (1988); and G.A. Schuler and T. Sjöstrand, The hadronic properties of the photon in γp interactions, *Phys. Lett.* **B 300** (1993) 169.

[9] E-691: J.C. Anjos *et al.*, Charm Photoproduction, *Phys. Rev. Lett.* **62** , 513 (1989).

[10] E-691: J.C. Anjos *et al.*, Photon-Gluon-Fusion Analysis of Charm Photoproduction, *Phys. Rev. Lett.* **65** , 2503 (1990).

[11] NA14/2: M.P. Alvarez *et al.*, Study of charm photoproduction mechanisms, *Z.Phys.* **C 60**, 53 (1993).

[12] NA14/2: M.P. Alvarez *et al.*, $D\overline{D}$ correlations in photoproduction, *Phys. Lett.* **B 278** (1992) 385.

[13] E-687: P.L. Frabetti *et al.*, Studies of $D\overline{D}$ Correlations in High Energy Photoproduction, *Phys. Lett.* **B 308** (1993) 193.

[14] E-687: R. Gardner *et al.*, Photoproproduction of Charmed Hadrons, FERMILAB-Conf-94/365-E, presented at DPF'94, Albuquerque, New Mexico, August, 1994.

[15] ZEUS: M. Derrick *et al.*, Study of $D^*(2010)^{\pm}$ Production in *ep* Collisions at HERA, DESY 95-013, February, 1995.

[16] H1: C. Kleinwort *et al.*, Studies of Charm Production with the H1 Detector at HERA and Observation of Elastic Vector Meson Photoprodcution at HERA, presented at ICHEP-94, Glasgow, August, 1994.